AIAA 81-1468R

Numerical Study of Staged Fuel Injection for Supersonic Combustion

Elizabeth H. Weidner* and J. Philip Drummond†
NASA Langley Research Center, Hampton, Virginia

A parametric study of staged (multiple) perpendicular fuel injector configurations has been conducted using a computer code that solves the two-dimensional elliptic Navier-Stokes equations. The program computes the turbulent mixing and reaction of hydrogen fuel and air and allows the study of separated regions of the flow immediately preceding and following the injectors. The validity of the code is demonstrated in a cold flow helium injection study with a single injector. Results are presented that describe the flowfield near opposing staged injectors over a range of parameters. Parameters that are varied include injector size, fuel split, and distance between injectors. Comparisons of the configurations are made to assess their mixing and potential flameholding qualities.

Nomenclature

c	= specific heat
e	= total internal energy per unit volume
e_s	= static internal energy per unit volume
f	= hydrogen mass fraction
L_ζ, L_η	= streamwise and transverse finite difference operator, respectively
Le	= Lewis number
M	= Mach number
$\dot{m}$	= mass flow rate
p	= pressure
Pr	= Prandtl number
q	= heat flux
Sc	= Schmidt number
T	= temperature
t	= time
Δt	= time increment
u,v	= streamwise and transverse velocity components
x,y	= streamwise and transverse physical coordinates
$\Delta x, \Delta y$	= increments in physical finite difference grid
ζ,η	= streamwise and transverse computational coordinates
$\Delta\zeta, \Delta\eta$	= increments in computational finite difference grid
γ	= ratio of specific heats
Γ	= mass diffusion coefficient
κ	= effective thermal conductivity
μ	= total viscosity
ρ	= density
σ	= normal stress
τ	= shear stress

Subscripts

i,j	= x and y grid indexes
nnx, nny	= maximum grid points in x and y directions
x	= in streamwise direction
y	= in transverse direction

Superscript

n	= time index

Presented as Paper 81-1468 at the AIAA/SAE/ASME 17th Joint Propulsion Conference, Colorado Springs, Colo., July 27-29, 1981; submitted Aug. 12, 1981; revision received Feb. 10, 1982. This paper is declared a work of the U.S. Government and therefore is in the public domain.

*Mathematician, Hypersonic Propulsion Branch, High-Speed Aerodynamics Division.

†Aerospace Engineer, Computational Methods Branch, High-Speed Aerodynamics Division. Member AIAA.

Introduction

THE concept of an airframe-integrated scramjet (Fig. 1) has evolved from efforts at the NASA Langley Research Center to design a propulsion system for hypersonic air-breathing aircraft. The entire undersurface of the aircraft serves as part of the propulsion system; the forebody performs a significant part of the inlet function by precompressing the air and the afterbody is used for additional expansion of the nozzle exhaust gases. The basic engine is divided into several identical rectangular modules, one of which is shown in Fig. 1 with the sidewall removed. Each module consists of an inlet where the compression process begun by the vehicle undersurface is continued, fuel injection struts that complete the compression and provide locations for the injection of gaseous hydrogen fuel, a combustor where the fuel and air are reacted, and a nozzle through which the reacted mixture is expanded. Gaseous hydrogen fuel is injected from the struts both parallel and perpendicular to the engine primary flow. Pependicular injection causes rapid fuel-air mixing and is used to some degree at all flight Mach numbers to promote reaction in the upstream portion of the combustor. When operating in a lower Mach number range (M = 4-5), parallel injection must be used extensively to slow the mixing process and prevent thermal choking.

Researchers conducting subscale engine tests of a scramjet engine module[1,2] have encountered both ignition and flameholding problems due to the small scale of the models, the relatively low static temperatures and pressures which can occur even at high simulated Mach numbers, and details of the configuration itself. There have been encouraging results, however, using staged (multiple) perpendicular fuel injectors.[2] Figure 2 shows pressure distribution data from Mach 7 engine tests. The cross section of the strut region given in the figure indicates generally where each wall pressure data point is taken. The plot shows pressure distributions for zero fuel, and single- and two-staged fuel injection. In both cases with fuel injection, there was no change in the inlet pressures which implied that there was no undesirable inlet-combustor coupling. For the single injector configuration, only slight increases in pressure over the zero-fuel level were obtained, indicating little reaction. With staged fuel injection much higher pressures were obtained, indicating significant reaction was taking place and, in fact, flameholding occurred.

The staged injector concept is diagrammed schematically in Fig. 3. Instead of injecting fuel from a single injector along each wall, gaseous hydrogen fuel is injected from two injectors. Typically, the jet of fuel from a perpendicular injector blocks the mainstream flow causing an adverse pressure

gradient which separates the turbulent boundary layer upstream of that injector. The thickened boundary layer results, first, in a separation shock and, finally, in a region of recirculation ahead of the injector. A bow shock that turns the flow over the injector forms just ahead of the fuel jet. There is also a region of subsonic separation and recirculation downstream of a perpendicular injector caused by the rapid expansion of the flow behind the fuel jet. With staged injection an interaction occurs between the two injectors producing a greater flowfield disturbance and a larger recirculating region than would occur for a single injector. This large region of separated flow should provide longer residence times for fuel and air resulting in an improved region for flameholding.

In order to achieve good flameholding capability in the scramjet engine, several perpendicular injector configurations are being considered. As a first step in learning about the effects of staged fuel injection, a two-dimensional parametric study of the flowfields near staged perpendicular injectors has been conducted using a computer program[3,4] developed to study such highly complex, elliptic flowfields. The program solves the elliptic compressible Navier-Stokes and species equations using the MacCormack[5] time-split algorithm. Turbulence is modeled with an algebraic eddy-viscosity model,[6] and chemistry is described by a complete reaction model.[4] Although this paper presents two-dimensional results that are not directly applicable to a real three-dimensional engine problem, they provide some insight into trends that can be expected in the three-dimensional case, and they show that this type of analysis can handle the very complex flowfields associated with staged perpendicular injection.

Analysis

Governing Equations

The flowfield near one or more perpendicular hydrogen fuel injectors is governed by the complete Navier-Stokes equations and one or more additional equations describing the species present in the flow. Written in conservation law form for a simple hydrogen-air system in two-dimensional rectangular coordinates, these equations in the absence of body forces can be expressed as

$$\frac{\partial U}{\partial t}+\frac{\partial F}{\partial x}+\frac{\partial G}{\partial y}=0 \tag{1}$$

where

$$U=\begin{Bmatrix}\rho\\ \rho u\\ \rho v\\ e\\ \rho f\end{Bmatrix} \tag{2}$$

$$F=\begin{Bmatrix}\rho u\\ \rho u^2+\sigma_x\\ \rho uv+\tau_{xy}\\ (e+\sigma_x)u+\tau_{yx}v+q_x\\ \rho uf+\dot{m}_x\end{Bmatrix} \tag{3}$$

$$G=\begin{Bmatrix}\rho v\\ \rho uv+\tau_{yx}\\ \rho v^2+\sigma_y\\ (e+\sigma_y)v+\tau_{xy}u+q_y\\ \rho vf+\dot{m}_y\end{Bmatrix} \tag{4}$$

and

$$\sigma_x=p-\lambda\left(\frac{\partial u}{\partial x}+\frac{\partial v}{\partial y}\right)-2\mu\frac{\partial u}{\partial x} \tag{5}$$

$$\tau_{xy}=\tau_{yx}=-\mu\left(\frac{\partial u}{\partial y}+\frac{\partial v}{\partial x}\right) \tag{6}$$

$$\sigma_y=p-\lambda\left(\frac{\partial u}{\partial x}+\frac{\partial v}{\partial y}\right)-2\mu\frac{\partial v}{\partial y} \tag{7}$$

$$\lambda=-\tfrac{2}{3}\mu \tag{8}$$

$$\kappa=\frac{\gamma\mu}{Pr} \tag{9}$$

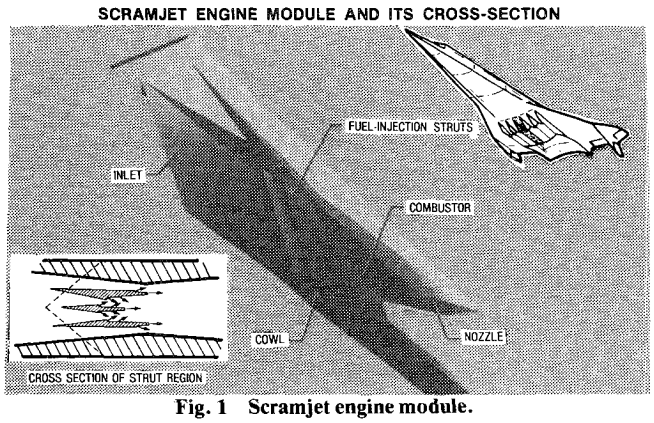

Fig. 1 Scramjet engine module.

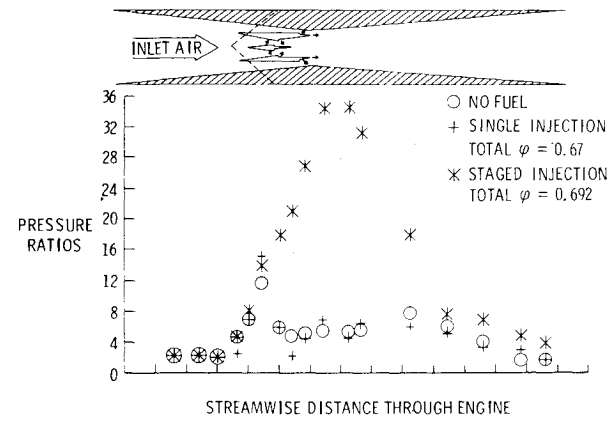

Fig. 2 Pressure distributions for zero fuel and single- and two-staged fuel injection.

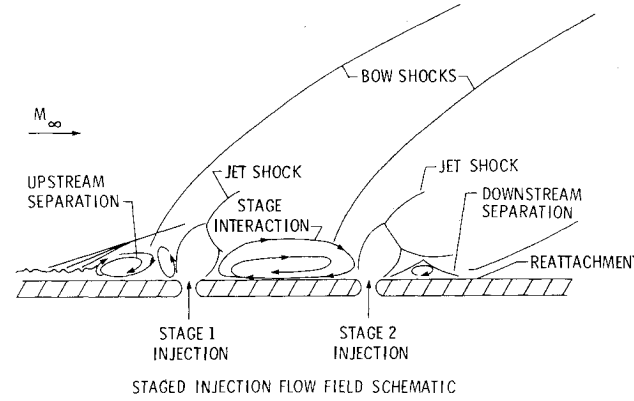

Fig. 3 Staged injection flowfield schematic.

$$\Gamma = \mu/Sc = \mu/Pr \qquad (Le=1) \tag{10}$$

$$\mu = \mu_{\text{laminar}} + \mu_{\text{turbulent}} \tag{11}$$

$$q_x = -\kappa \frac{\partial e_s}{\partial x} \tag{12}$$

$$q_y = -\kappa \frac{\partial e_s}{\partial y} \tag{13}$$

$$\dot{m}_x = -\Gamma \frac{\partial f}{\partial x} \tag{14}$$

$$\dot{m}_y = -\Gamma \frac{\partial f}{\partial y} \tag{15}$$

$$e_s = \int_0^T c\,\mathrm{d}T = \bar{c}T \tag{16}$$

$$\bar{c} = \int_0^T c\,\mathrm{d}T/T \tag{17}$$

The specific heat is a function of the local temperature and species concentrations. The pressure is calculated from the equation of state; and the laminar viscosity is calculated from Sutherland's law. The turbulent viscosity is calculated from an algebraic eddy viscosity model developed for use with flows that contain flow separation.[6]

Solution of the Governing Equations

An algebraic coordinate transformation[7] is used to transform the independent variables (x,y) from a nonuniform grid in the physical domain to a uniform grid in the computational domain with variables (ζ,η). Intermediate functions, $\bar{\zeta}=\bar{\zeta}(\zeta)$ and $\bar{\eta}=\bar{\eta}(\eta)$ (Fig. 4), can be defined to obtain the compression of the grid needed in both the x and y directions to resolve high gradients near walls and fuel injectors. After applying the transformation, Eq. (1) can be expressed as

$$\frac{\partial U}{\partial t} + \frac{\partial F}{\partial \zeta}\frac{\partial \zeta}{\partial x} + \frac{\partial F}{\partial \eta}\frac{\partial \eta}{\partial x} + \frac{\partial G}{\partial \zeta}\frac{\partial \zeta}{\partial y} + \frac{\partial G}{\partial \eta}\frac{\partial \eta}{\partial y} = 0 \tag{18}$$

Equations (2-15) tranform from the physical to the computational domain in similar fashion.

The time-split finite difference technique of MacCormack[5] is used to integrate the transformed governing equations until a steady-state solution is reached. If a solution to Eq. (18) is known at some time $t=n\Delta t$, the solution at the next time step, $t=(n+1)\Delta t$, can be calculated from

$$U_{i,j}^{n+1} = L(\Delta t)\, U_{i,j}^{n} \tag{19}$$

for each node point (i,j) in the finite difference grid of the computational domain. The finite difference operator L is split into two one-dimensional difference operators $L_\zeta(\Delta t)$ and $L_\eta(\Delta t)$, and each split operator consists of a predictor and corrector integration step. The one-dimensional operators are combined to form a two-dimensional operator through the symmetric operator sequence

$$L(\Delta t) = L_\eta(\Delta t/2)\, L_\zeta(\Delta t)\, L_\eta(\Delta t/2) \tag{20}$$

One pass through Eq. (20) advances the finite difference form of Eq. (18) through one time step, Δt.

Boundary Condition

No-slip conditions along the lower wall require that

$$u_{i,1} = 0 \tag{21}$$

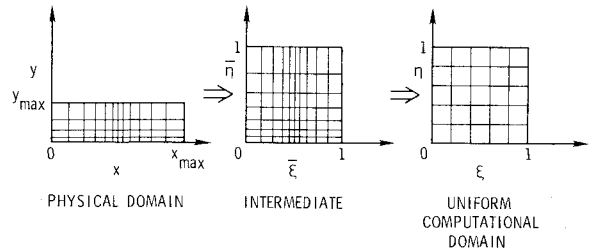

Fig. 4 Domains in coordinate transformation.

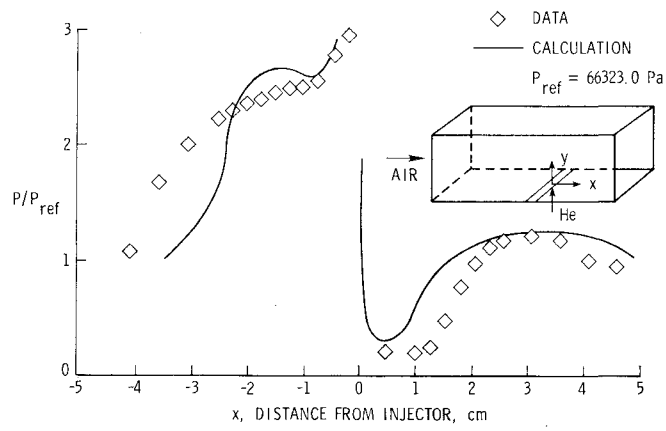

Fig. 5 Comparison of experimental and computed wall pressures.

$$v_{i,1} = 0 \tag{22}$$

The wall is assumed to be adiabatic so that the normal derivative of temperature must vanish giving

$$T_{i,1} = T_{i,2} \tag{23}$$

The normal derivative of the total hydrogen mass fraction must also vanish along the adiabatic wall giving

$$f_{i,1} = f_{i,2} \tag{24}$$

Pressure is determined from the normal momentum equation, and the density is calculated from the ideal gas law. At the hydrogen fuel injectors the dependent variables are fixed at their initial values consistent with the required physical behavior of the jets.

Along a plane of symmetry, the normal derivative of the u velocity is required to vanish so that

$$u_{i,nny} = u_{i,nny-1} \qquad v_{i,nny} = 0 \tag{25}$$

Boundary conditions along the supersonic inflow plane are specified by holding the velocities, temperature, pressure, and mass fraction fixed at their initial values and then calculating the density and total internal energy. Along the supersonic outflow plane the dependent variables are set equal to their values at the preceding streamwise node with the exception of density and total internal energy which are calculated again.

Chemistry Model

The chemical reaction of hydrogen fuel and air is modeled in the present work using a complete reaction model.[4] This model assumes that reaction must occur at any point where both fuel and air are present. The extent of reaction is determined by the stoichiometric limit of the hydrogen-air reaction; i.e., the amount of hydrogen present determines the extent of reaction with a fuel-lean condition, and the amount of oxygen present determines the extent of reaction with a

fuel-rich condition. Reaction is inhibited at a point only by a 4% by mass of hydrogen flammability limit criterion.

The chemistry model is applied at the end of each computational time step. Once the new composition (hydrogen, oxygen, nitrogen, and water) is known, a new temperature is determined at each computational node, and the gas mixture properties are recomputed. The calculation then proceeds to a new time step.

Results

Before applying the program to the staged injection problem, its ability to compute such flows is assessed here by comparing calculations with a recent experiment by G. O. Kraemer and R. C. Rogers to study details of the flowfield near a slot sonically injecting helium transversely into a ducted supersonic airstream. Results from a parameter study of staged perpendicular injection are then given.

Program Verification

An experiment has been conducted specifically to provide data for evaluation of the computer code. The experimental apparatus is shown in the insert on Fig. 5. In the experiment, helium was injected at sonic conditions from a 0.0559-cm slot into a rectangular duct 7.62-cm high and 25.4-cm long. The slot was located 17.8-cm downstream of the duct entrance. Pressure and helium volume fraction were measured along the lower wall with wall taps located both upstream and downstream of the slot, and cross-stream surveys of pressure and helium volume fraction were also made by probe rakes at several stations downstream of the slot. The flow in the duct was assumed to be turbulent throughout.

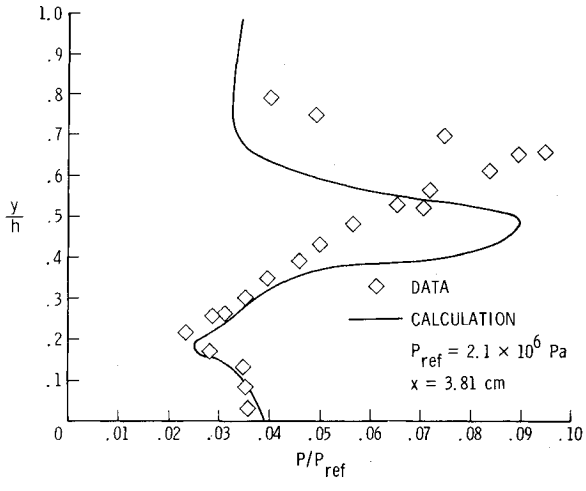

Fig. 6 Comparison of experimental and computed static pressures.

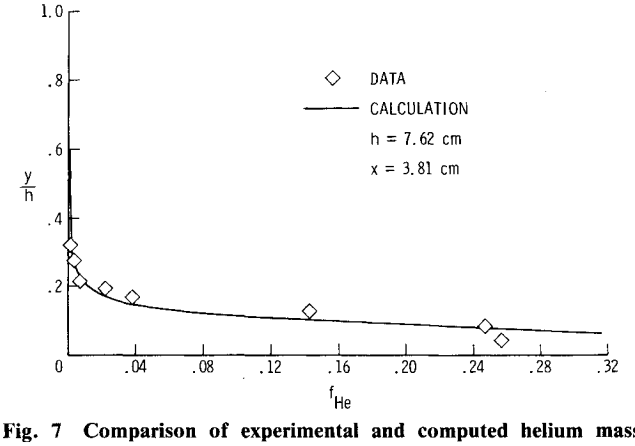

Fig. 7 Comparison of experimental and computed helium mass fractions.

The conditions of the helium at the slot exit were $M=1.0$, $T=217$ K, and $p=1.24$ MPa. The conditions of the air at the entrance to the duct were $M=2.9$, $T=108$ K, and $p=0.0663$ MPa. These conditions were held fixed during the course of the calculation. The physical domain was spanned by a finite difference grid with 110 nodes in the streamwise direction and 51 nodes in the transverse direction. The grid was compressed in both a streamwise direction near the injector and in a transverse direction near the upper and lower walls.

Results are given in Figs. 5-7. Figure 5 shows a comparison of the experimental and computed results for wall pressure upstream and downstream of the injector which is located at $x=0$. The computed results agree fairly well with the data. Both show a pressure rise associated with the upstream separated region, a plateau region, and then another rise close to the injector. The initiation of the pressure rise upstream of the injector is underpredicted by about 0.75 cm and lags the experimental values until a point about 2.5-cm upstream of the slot is reached. The agreement is reasonably good in the plateau region (-2.5 cm $\leq x \leq -0.75$ cm) and also in the region interior to the plateau (-0.75 cm $\leq x \leq 0.0$) where the pressure begins to increase again. The pressure is somewhat overpredicted downstream of the injector, but still agrees reasonably well with the data. Underprediction of the beginning of the initial pressure rise is likely caused by failure to completely resolve the turbulent boundary layer present limiting the upstream influence of the separation ahead of the injector. Boundary-layer resolution may have been inhibited by grid coarseness near the wall and the algebraic turbulence model. Similar problems are also likely to occur around the separated region downstream of the injector.

Figure 6 shows experimental data from a static pressure survey 3.8-cm downstream of the injector and computed cross-stream static pressures at the same location in the duct. The agreement of the data and the computation is quite good near the lower wall and continues to be reasonably good out to about 0.4 duct height. Beyond that point the pressure rise and peak associated with the separation and bow shocks are predicted to occur closer to the lower wall than the experiment indicates. Recall that the flow separation ahead of the slot occurs further downstream in the analysis than in the experiment. This would cause the separation and bow shocks to shift further downstream as well, such that they would be closer to the lower wall along with the associated pressure rises. Figure 7 shows a comparison of the measured and computed helium mass fractions also at the 3.8-cm station downstream of the injector. The agreement between the experiment and program calculations is quite good at all locations except very near the lower wall.

Overall, the data-theory comparisons for this case appear to be good considering that the transverse jet flowfield is very complex, and these are "predictive"-type calculations. No attempt has been made to adjust the turbulence model, constants, grid, or other parameters to accomplish a better comparison. These calculations and prior comparisons with other data[3,4] support the validity of using the code for a parametric study of staged fuel injection.

Parametric Study

Parametric calculations have been performed for two injector sizes, widths of 0.0635 and 0.127 cm, and two fuel splits at varying distances between the injectors (see Table 1). For one fuel split, 20% by mass of hydrogen was injected from the upstream injector and 80% from the downstream jet; these were then reversed to give an 80/20 fuel split. In order to make meaningful comparisons, all the cases in the parametric study were run on a rectangular duct 8-cm high with the inlet conditions: $M=2.7$, $T=800$ K, and $p=0.101$ MPa. Gaseous hydrogen fuel was injected from opposing slot injectors at $M=1.1$ and $T=242$ K with pressures at the jets being determined by the slot widths and fuel split to maintain

Table 1 Cases in parametric study

Case	Injector width, cm	Injector Spacing, cm	Fuel split % Upstream	% Downstream	Pressure upstream	Ratio at jet downstream
1	0.127	—	100	—	10	—
2	0.0635	1.27	20	80	4	16
3	0.0635	1.27	80	20	16	4
4	0.127	1.27	20	80	2	8
5	0.127	1.27	80	20	8	2
6	0.0635	2.54	20	80	4	16
7	0.0635	2.54	80	20	16	4
8	0.127	2.54	20	80	2	8
9	0.127	2.54	80	20	8	2
10	0.127	5.08	20	80	2	8
11	0.127	7.62	20	80	2	8
12	0.127	15.24	20	80	2	8
13	0.127	15.24	80	20	8	2
14	0.0635	15.24	20	80	4	16
15	0.127	15.24	20	80	2	8

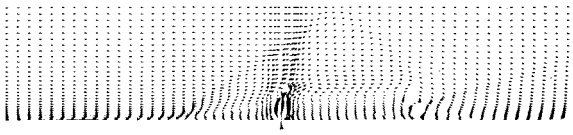

Fig. 8 Velocity vector field in lower half duct for a single injector, 0.127-cm wide (case 1).

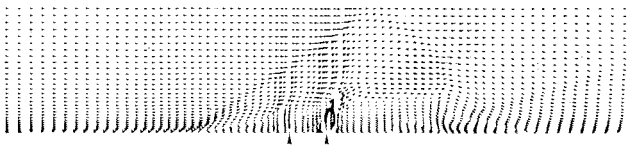

Fig. 9 Velocity vector field in lower half duct for staged injectors spaced 1.27-cm apart (case 4).

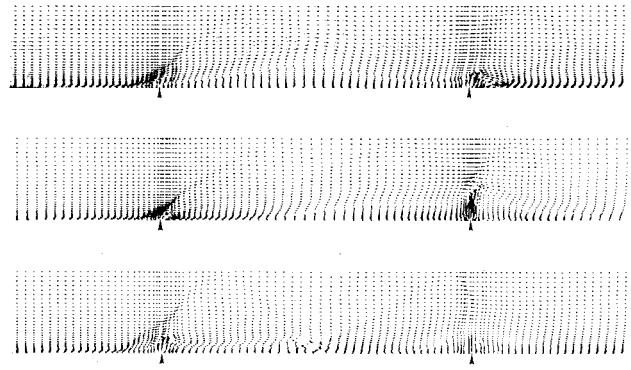

Fig. 10 Velocity vector field in lower half duct for staged injectors spaced 15.24-cm apart; a) slot width = 0.127 cm, 20/80 fuel split (case 12); b) slot width = 0.0635 cm, 20/80 fuel split (case 14); and c) slot width = 0.127 cm, 80/20 fuel split (case 13).

a fuel equivalence ratio of 0.5. Because of symmetry about the duct centerline, calculations were performed only between the lower wall and the centerline.

Most of the cases (Table 1, 1-11) were run with a 20-cm-long duct segment. When the distance between the injectors was increased to 15.24 cm, however, the duct length was increased to 30 cm to completely capture the disturbance. In all cases the finite-difference grid in the transverse direction contained 30 nodes with compression near the lower wall. The streamwise grid size varied from 67 nodes for case 1 to 109 nodes for case 14. The streamwise grid was compressed near the fuel injectors. Case 15 in Table 1 is the only case in which chemical reaction was computed; all other cases considered only mixing of hydrogen fuel and air. It took an average of 30,000 time steps to reach steady state, requiring approximately 1½ h on a Control Data Cyber-203.

Characteristics of the nonreacting flowfields for several cases are shown in the plots of the velocity vectors (Figs. 8-10). Direction of the arrows indicates flow direction and arrow length indicates relative velocity. In each case, the separated regions upstream of the first injector, between the two injectors and downstream of the second injector, are indicated by a reversal of the velocity vectors as they form a recirculation pattern. The separation and bow shocks that turn the mainstream flow over the injectors are quite strong and can be seen in the upward deflection of the velocity vectors ahead of the first injector. The downrunning bow shock from the upper injectors (actually, in these cases, a reflection of the uprunning shock from the centerline) can be seen as the velocity vectors turn downward from the centerline just beyond the point where the shock strikes it.

The overall disturbance to the flowfield caused by a single injector (Fig. 8) is not greatly different from that caused by staged injectors with a 1.27-cm spacing (Fig. 9), the primary difference being a small recirculating region between the jets. The separation and bow shocks associated with the two injectors appear to merge into a single shock which strikes the centerline and is reflected downstream of the second injector. As the injector spacing is increased, the recirculating region between the injectors gets progressively larger and the shock and its reflection move progressively further upstream. It is not until the injector spacing reaches 15.24 cm that the reflected shock strikes ahead of the second injector (Fig. 10a). (Note the change in scale from the previous vector plots due to the increased duct length.) The recirculating region between the jets is quite large in both the streamwise and transverse directions, and the velocity in this region is mostly subsonic.

It is only at this widest spacing that changing fuel split and injector size cause significant differences in the flowfield. The differences caused by changing slot widths at the closer spacings are almost imperceptible, but at the widest spacing a smaller injector size and higher injectant pressure results in a smaller recirculating region between the jets (Fig. 10b). At injector spacings less than 15.24 cm the 80/20 fuel split causes the shock to strike the centerline slightly upstream of where the shock strikes for the 20/80 split. For an 80/20 split at the widest spacing the flow actually reattaches between the jets (Fig 10c), resulting in two recirculation zones in that region. Based on the size of the recirculation zone, the best region for flameholding appears to occur when the injectors are 0.127-cm wide, spaced 15.24 cm apart and the fuel split is 20/80 (Table 1, case 12).

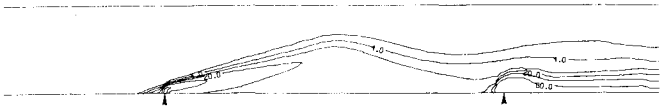

Fig. 11 Hydrogen mass fraction contours in lower half duct (case 12).

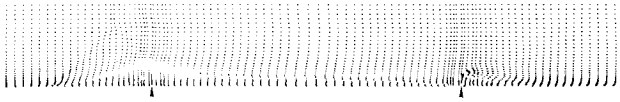

Fig. 12 Velocity vector field in lower half duct for staged injection with reaction (case 15).

A contour map of the hydrogen mass fraction distribution for case 12 is shown in Fig. 11. Contour lines are plotted for 80, 40, 20, 10, 4, and 1% by mass of hydrogen. The fuel penetrates well into the mainstream, and there is good mixing of the fuel and air in the region between the injectors where the velocity of the flow (Fig. 10a) is very low. The combination of good mixing and long residence time should provide an excellent region for flameholding.

To complete this analysis, case 12 was considered with chemical reaction. The velocity vector field for the reacting flow (case 15) is shown in Fig. 12. Comparing with the corresponding nonreacting flow (Fig. 10a) it can be seen that chemical reaction has a significant effect on the flowfield. With reaction, the overall penetration into the primary flow of the recirculating region between the injectors is lessened, and the separation and bow shocks associated with the first injector initiate further upstream. Expected changes in pressure and temperature also occur; the maximum pressure in the duct is about 34% higher with reaction, and the maximum temperature is increased by about 88%. Chemical reaction also introduces the possibility of thermal choking. The significant differences between the reacting and nonreacting flowfields reinforce the importance of considering chemical reaction when a complete analysis of orifice-staged fuel injectors is performed.

Concluding Remarks

A parametric study of potential perpendicular fuel injector configurations for a scramjet engine has been conducted using a two-dimensional computer program which has been developed to model these configurations and their associated flowfields. The program was first compared with some recent experimental data to allow assessment of the modeling that was used. The parametric study was then carried out with the program using identical modeling. Parameters varied in the parametric study included the distance between the injectors, the injector width, and the fuel split between the injectors. It was found that the distance between the injectors had to be relatively large (15.24 cm) before there were significant differences in the flowfields. Until the distance between the injectors reached that point, changes in injector size and fuel split did not have a significant effect. In all cases the flowfields showed a great deal of sensitivity to the location of the shocks. The best region for flameholding appeared to occur at the widest spacing with the larger injector size and a fuel split such that most of the fuel was injected from the downstream injector. When chemical reaction was considered in this case the flowfield was considerably different from the nonreacting flow.

The current work shows that the two-dimensional Navier-Stokes code is capable of handling the complex flowfields produced by staged fuel injectors, and is sufficiently accurate to be used for a parametric study. This work represents an intermediate step in obtaining a complete analysis of staged fuel injection in a scramjet engine. The simple chemistry model needs improvement toward the use of a finite rate chemistry model in order to show the kinetic effects of improved residence time on ignition and reaction. As better turbulence models become available they will be used, and the program will be extended to three dimensions to model orifice injectors. The trends presented here indicate that the three-dimensional version of the code, when it is available, should be a useful tool in designing optimal staged injector configurations for the Langley scramjet engine.

References

[1] Guy, R. W. and Mackley, E. A., "Initial Wind Tunnel Tests at Mach 4 and 7 of a Hydrogen-Burning Airframe-Integrated Scramjet," AIAA Paper 79-7045, April 1979.

[2] Beach, H. L. Jr., Mackley, E. A., Rogers, R. C., and Chinitz, W., "Use of Silane in Scramjet Research," 17th JANNAF Combustion Meeting, Hampton, Va., Sept. 1980.

[3] Drummond, J. P., "Numerical Investigation of the Perpendicular Injector Flow Field in a Hydrogen Fueled Scramjet," AIAA Paper 79-1482, July 1979.

[4] Drummond, J. P. and Weidner, E. H., "Numerical Study of a Scramjet Engine Flow Field," AIAA Paper 81-0186, Jan. 1981.

[5] MacCormack, R. W. and Baldwin, B. S., "A Numerical Method for Solving the Navier-Stokes Equations with Application to Shock-Boundary Layer Interactions," AIAA Paper 75-1, Jan. 1975.

[6] Baldwin, B. S. and Lomax, H., "Thin Layer Approximations and Algebraic Model for Separated Turbulent Flows," AIAA Paper 78-257, Jan. 1978.

[7] Smith, R. E. and Weigel, B. L., "Analytic and Approximate Boundary Fitted Coordinate Systems for Fluid Flow Simulation," AIAA Paper 80-0192, Jan. 1980.